

# Measurement of $\tan\beta$ in associated $tH^\pm$ production in $\gamma\gamma$ collisions

M. A. Doncheski

*Department of Physics, Pennsylvania State University, Mont Alto, Pennsylvania 17237, USA*

Stephen Godfrey

*Ottawa-Carleton Institute for Physics, Department of Physics, Carleton University, Ottawa, Canada K1S 5B6,  
Special Research Centre for the Subatomic Structure of Matter, University of Adelaide, Adelaide South Australia 5000, Australia,  
and TRIUMF, 4004 Wesbrook Mall, Vancouver B.C., Canada V6T 2A3*

Shouhua Zhu

*Ottawa-Carleton Institute for Physics, Department of Physics, Carleton University, Ottawa, Canada K1S 5B6*

(Received 16 June 2003; published 3 September 2003)

The ratio of neutral Higgs field vacuum expectation values,  $\tan\beta$ , is one of the most important parameters to determine in type-II two Higgs doublet models, specifically the minimal supersymmetric standard model. Assuming the energies and integrated luminosity of a future high energy  $e^+e^-$  linear collider of  $\sqrt{s}=500, 800, 1000, \text{ and } 1500$  GeV and  $\mathcal{L}=1 \text{ ab}^{-1}$  we show that associated  $tH^\pm$  production in  $\gamma\gamma$  collisions can be used to make an accurate determination of  $\tan\beta$  for low and high  $\tan\beta$  by precision measurements of the  $\gamma\gamma \rightarrow H^\pm t + X$  cross section.

DOI: 10.1103/PhysRevD.68.053001

PACS number(s): 12.15.Ji, 12.60.Cn, 14.70.-e, 14.80.-j

## I. INTRODUCTION

A fundamental open question of the standard model (SM) is the origin of electroweak symmetry breaking (EWSB) [1,2]. The simplest description of EWSB results in one neutral scalar particle which, however, has well known problems associated with it. *A priori*, a more complicated Higgs sector is phenomenologically just as viable [3]. The next simplest case is the general two Higgs doublet model (2HDM). A constrained version of the 2HDM is a part of the minimal supersymmetric extension of the SM (MSSM) [4,5] where spontaneous symmetry breaking is induced by two complex Higgs doublets and leads to five physical scalars: the neutral *CP*-even  $h^0$  and  $H^0$  bosons, the neutral *CP*-odd  $A^0$  boson, and the charged  $H^\pm$  bosons. At the tree level the MSSM Higgs sector has two free parameters which are usually taken to be the ratio of the vacuum expectation values of the two Higgs doublets,  $\tan\beta=v_2/v_1$ , where  $v_2$  couples to the up-type quarks and  $v_1$  to the down-type quarks, and the mass of the  $A^0$  boson,  $m_A$ . The elucidation of EWSB is the primary goal of the Large Hadron Collider (LHC) at CERN and the proposed high energy  $e^+e^-$  Linear Collider (LC) [6–13].

The ratio of neutral Higgs field vacuum expectation values,  $\tan\beta$ , is a key parameter needed to be determined in type-II two Higgs doublet models and the MSSM. In addition to providing information about the structure of the non-minimal Higgs sector, the measurement of this parameter also provides an important check of supersymmetry structure as this parameter also enters the chargino, neutralino, and third generation squark matrices and couplings [14]. Nevertheless, the Yukawa couplings of Higgs bosons are the most direct way to probe the structure of the vacuum state of these theories. To address this issue a number of recent studies have examined how one could measure  $\tan\beta$  at the LHC [15] and future high energy  $e^+e^-$  colliders [16–21]. A  $\gamma\gamma$  “Compton collider” option, from backscattered laser light

off of highly energetic electron beams, has been advocated as a valuable part of the linear collider program which could make crucial measurements of the Higgs sector [22]. If charged Higgs bosons were observed, cross section measurements could potentially give information about the underlying theory. Analysis of the process  $e^+e^- \rightarrow H^+H^-$  indicates that the absolute event rate and ratios of branching ratios in various  $H^+H^-$  final state channels will allow a relatively accurate determination of  $\tan\beta$  at low  $\tan\beta$  [13]. The branching ratios for  $H$ ,  $A$ , and  $H^\pm$  are sensitive to  $\tan\beta$  when  $\tan\beta$  is less than roughly 20 so that a precise measurement of branching ratios can give a good determination of  $\tan\beta$ .

Another possibility for measuring  $\tan\beta$  is associated  $tH^\pm$  production in  $\gamma\gamma$  collisions [23]. The subprocess  $b\gamma \rightarrow H^- t$  proceeds via  $b\gamma$  fusion and utilizes the  $b$ -quark content of the photon. Despite the fact that there is good agreement on the  $b$ -quark content of the photon between the existing sets of photon parton distribution functions, at this time there are no experimental data to back up the theoretical calculations. This is not an insurmountable problem. A direct measurement of the  $b$ -quark content of the photon is possible in a linear  $e^+e^-$  or  $e\gamma$  collider (see for example Ref. [24]) and such a measurement will need to be made before, and independently of, the process discussed in this paper. In this paper we study how well the subprocess  $b\gamma \rightarrow H^- t$  can be used to measure  $\tan\beta$ . We find that it can be used to make a good determination of  $\tan\beta$  for most of the parameter space with the exception of the region around  $\tan\beta \approx 7$ . As such, it is a useful complement to other measurements for studying  $\tan\beta$  [18].

## II. CALCULATIONS AND RESULTS

The process  $\gamma\gamma \rightarrow tH^\pm + X$  makes use of the  $tbH^\pm$  interaction to measure  $\tan\beta$ . The interaction is given by [25,26]

$$i \frac{V_{tb}}{\sqrt{2}v} [m_b \tan \beta (1 + \gamma_5) + m_t \cot \beta (1 - \gamma_5)]. \quad (1)$$

To calculate the process  $\gamma\gamma \rightarrow H^- t + X$  we calculate the subprocess  $\gamma b \rightarrow H^- t$  and convolute it with the  $b$  distribution in the photon. This is illustrated in Fig. 1. It has been shown that this is a reasonable approximation for the energies and kinematic regions we are considering in this paper [24]. The amplitude squared for the subprocess  $b\gamma \rightarrow tH^-$  is given by

$$\begin{aligned} \sum |M(b\gamma \rightarrow tH^\pm)|^2 = & 8\sqrt{2}G_F\pi\alpha(m_b^2\tan^2\beta + m_t^2/\tan^2\beta) \left\{ \frac{Q_b^2}{s^2} 2p_t \cdot p_\gamma p_b \cdot p_\gamma - \frac{Q_t^2}{(t-m_t^2)^2} 2[m_t^2(p_b \cdot p_t - p_b \cdot p_\gamma) - p_t \cdot p_\gamma p_b \cdot p_\gamma] \right. \\ & - \frac{2}{(u-m_t^2)^2} 2p_t \cdot p_b (m_t^2 - 2p_b \cdot p_t) - 2 \frac{Q_b Q_t}{s(u-M_h^2)} [2(p_t \cdot p_b + p_t \cdot p_\gamma)(p_t \cdot p_b - p_b \cdot p_\gamma) - m_t^2 p_b \cdot p_\gamma] \\ & - 2 \frac{Q_b}{s(u-M_h^2)} [2p_t \cdot p_b (p_b \cdot p_t + p_t \cdot p_\gamma) - m_t^2 p_b \cdot p_\gamma] + \frac{Q_t}{(t-m_t^2)(u-M_h^2)} \\ & \left. \times [2p_t \cdot p_b (p_t \cdot p_b - p_b \cdot p_\gamma) + m_t^2 (p_b \cdot p_\gamma - 2p_t \cdot p_b)] \right\}. \quad (2) \end{aligned}$$

In our numerical results we include an additional factor of 2 from producing either an  $H^+$  or  $H^-$  and a factor of 2 because the  $b$ -quark can come from either initial photon. We note that we are ignoring  $m_b$  compared to  $m_t$  and  $M_H$  everywhere except in the coupling factor where  $m_b \tan \beta$  can be comparable to  $m_t/\tan \beta$ . To obtain the subprocess cross section we integrate the matrix element using Monte Carlo integration [26] and convolute the subprocess with the  $b$ -quark distribution in the photon and the photon spectrum, either the energy distribution obtained from backscattering a laser from an electron beam [27] or the Weizsäcker-Williams distribution [28]. The cross sections are found by evaluating the following expression:

$$\sigma = \int dx_1 dx_2 dx_3 f_{\gamma/e}(x_1) f_{\gamma/e}(x_2) f_{b/\gamma}(x_3) \hat{\sigma}(\hat{s}) \quad (3)$$

where  $\hat{\sigma}(\hat{s})$  is the subprocess cross section for center of mass energy  $\sqrt{\hat{s}}$ . We have only included tree-level contributions and are aware that higher order corrections are likely to be non-negligible. Nevertheless, we feel that our approach is satisfactory for a preliminary study to gauge the potential of this process for measuring  $\tan \beta$ . Our calculations have explicit dependence on the  $b$  and  $t$ -quark masses. We take  $m_b = 4.4$  GeV,  $m_t = 175$  GeV, and  $V_{tb} \sim 1$ . In addition, we used  $M_W = 80.41$  GeV,  $G_F = 1.166 \times 10^{-5}$  GeV $^{-2}$ , and  $\alpha = 1.0/128.0$  [29]. To obtain numerical results we used the

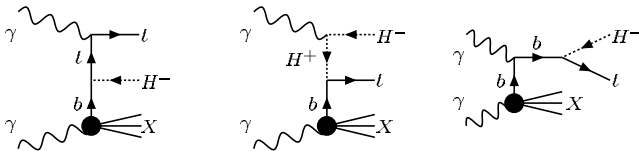


FIG. 1. Feynman diagrams for the process  $\gamma\gamma \rightarrow tH^- + X$  proceeding via the  $b$ -quark content of the photon.

Glück-Reya-Vogt (GRV) distributions [30]. Other distributions are available [31,32] and with recent LEP and HERA data, updates are forthcoming [33]. The cross section is shown in Fig. 2 as a function of  $M_H$  for  $\sqrt{s} = 500$  GeV for  $\tan \beta = 1.5, 3, 7, 30,$  and  $40$ .

The process we are studying has two initial state photons. In addition to the backscattered laser photons the initial state photons can also be Weizsäcker-Williams photons bremsstrahlung from the initial electron beams so that in addition to  $\gamma\gamma$  collisions we also consider  $e\gamma$  and  $e^+e^-$  collisions. We show the cross sections for the  $\gamma\gamma$ ,  $e\gamma$  and  $e^+e^-$  modes in Fig. 3 for  $\tan \beta = 3$  and  $40$ . One sees that the cross sections decrease by about an order of magnitude for each replacement of backscattered laser photons with Weizsäcker-Williams photons although the cross sections for

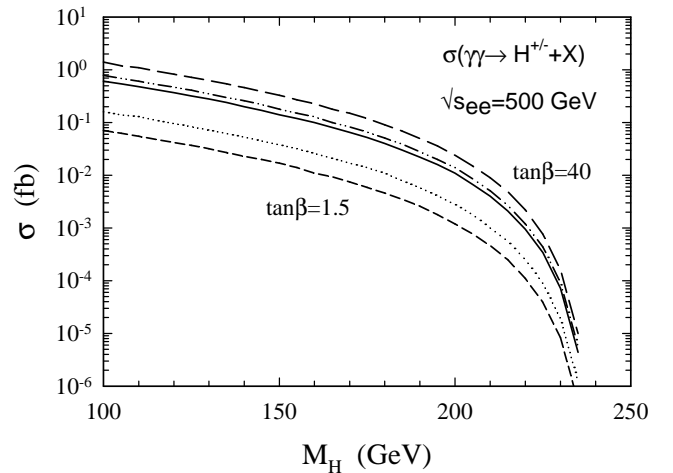


FIG. 2.  $\sigma(\gamma\gamma \rightarrow tH^- + X)$  for the  $\gamma\gamma$  backscattered laser case with  $\sqrt{s_{ee}} = 500$  GeV and  $\tan \beta = 1.5$  (short-dashed line), 3 (dotted line), 7 (solid line), 30 (dot-dot-dashed line), and 40 (long-dashed line).

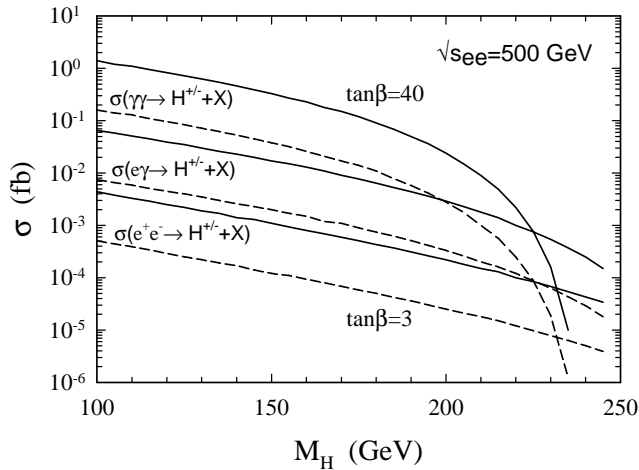


FIG. 3.  $\sigma(\gamma\gamma \rightarrow tH^\pm + X)$  for the  $\gamma\gamma$ ,  $e\gamma$  and  $e^+e^-$  cases with  $\sqrt{s_{ee}} = 500$  GeV and for  $\tan\beta = 3$  (dashed lines) and 40 (solid lines). For each set the largest cross section is for the  $\gamma\gamma$  case, the middle cross section for the  $e\gamma$  case and the smallest cross section for the  $e^+e^-$  case.

backscattered laser photons give lower kinematic limits due to the cutoff in their energy spectrum. Because good statistics are central to extracting precision measurements of  $\tan\beta$  we find that the error increases substantially for the  $e\gamma$  and  $e^+e^-$  cases compared to the  $\gamma\gamma$  case.

This is a preliminary analysis; as such we do not explicitly consider detector efficiencies nor include backgrounds. They are taken into account by assuming different values for the overall detection efficiency which we discuss below. Additionally, we do not include decay branching ratios. The branching ratios are well known [34,35], and dominated by  $t\bar{b}$  or  $\tau\nu_\tau$  depending on the  $H^\pm$  mass and  $\tan\beta$ .

A precise measurement of  $\tan\beta$  depends on a precise measurement of the  $tH^\pm$  production cross section. Thus, the issue of extracting the event signal from backgrounds and the efficiency with which this can be accomplished becomes the determining factor in the  $\tan\beta$  measurement. The most significant backgrounds which need to be separated out are  $\gamma\gamma \rightarrow t\bar{t}$  and  $\gamma\gamma \rightarrow t\bar{b} + \bar{t}b$  (where one of the  $b$ 's is lost down the beam) and  $\gamma\gamma \rightarrow t\bar{b} + W^-$  (where the  $b$  is lost down the beam and the  $W$  decays to  $\tau + \bar{\nu}_\tau$ ). The final state, and thus the most significant background, depends on the mass,  $M_{H^\pm}$ . If  $M_{H^\pm} > m_t$ ,  $H^\pm \rightarrow t\bar{b}$  will be the dominant decay mode and if  $M_{H^\pm} < m_t$ ,  $H^\pm \rightarrow \tau\nu$  will be the dominant decay mode. In either case, these backgrounds can be distinguished from the signal by reconstructing the final states.

For the case that  $M_{H^\pm} > m_t$  there will be two  $t$ -quarks in the final state. Each of the  $t$ -quarks will decay to  $bW$  with the  $W$ 's subsequently decaying to either  $q\bar{q}$  ( $jj$ ) or  $\ell\nu$  final states. The hadronic  $W$  decays lead to three jets in the final state while the leptonic  $W$  decay leads to one jet, an isolated lepton and missing energy. To reconstruct the event one needs to associate the final state jets, leptons, and missing energy with the originating parton.  $b$ -tagging is crucial to reconstructing the event and there is a tradeoff of efficiency versus mistagging a  $c$  or  $uds$  jet. The  $W$  is reconstructed from

the non- $b$ -tagged jets and the  $t$  is reconstructed through a constrained fit to the  $W$  and the  $b$ -jet that gives the best fit to the  $t$ -quark mass. For leptonic  $W$  decay the longitudinal component of the neutrino momentum can be fixed using the  $W$  mass constraint with the missing transverse momentum. The remaining  $b$ -jet is paired with the reconstructed top to reconstruct the  $H^\pm$ . As it is not possible to know which of the two top quarks originates from the Higgs decay there is a large combinatorial background from signal events and the associated difficulty in assigning non- $b$  jets to the correct top cluster. However, the constrained kinematic fits can be used to distinguish between the signal and background. After imposing selection criteria signal events can be selected with some efficiency but with some fraction of the events misidentified background.

For the case  $M_{H^\pm} < m_t$  the final state will consist of a charged  $\tau$ -lepton, a  $\tau$ -neutrino and a  $t$ -quark, which will lead to 0, 1 or 2 charged leptons, missing  $E_T$  and at least one jet. As above, the  $t$ -quark can be reconstructed from the  $b$ -tagged jet and hadronic or leptonic  $W$  decay products, with some efficiency and some probability of misidentification. Given the success of the LEP Collaborations in measuring  $\tau$  properties, for example the  $\tau$  lifetime [36] and polarization [37–40],  $\tau$ -leptons can be reconstructed successfully in a collider environment. The  $\tau$ -lepton can be reconstructed from low multiplicity, collimated (one-prong) hadronic decays, with the  $\tau$  mass constraint determining the transverse momentum of the  $\nu_\tau$  produced in the  $\tau$  decay. Such single prong decays account for approximately 46% of all  $\tau$  decays [ $Br(\tau \rightarrow \pi\nu) \sim 12\%$ ,  $Br(\tau \rightarrow \rho\nu) \sim 26\%$  and  $Br(\tau \rightarrow a_1\nu) \sim 8\%$ ]. As noted above, LEP Collaborations have been successful in reconstructing  $\tau$  events; for example, ALEPH [37] report 60–80% efficiency in reconstructing single prong  $\tau$  decays, with misidentification generally between 4–20%. ALEPH report on two  $\tau$  identification techniques, one with higher efficiency but higher misidentification probability than the other. This is a generic property of  $\tau$  reconstruction. Other LEP Collaborations report similar efficiencies and sample purities [38–40]. Leptonic  $\tau$  decays, on the other hand, have two neutrinos, each carrying transverse momentum, making the full reconstruction of the  $\tau$  problematic. Furthermore, the measurement considered here is going to be made after the discovery and measurement of the charged Higgs boson, so the Higgs boson mass can be used to constrain the transverse momentum of the  $\nu_\tau$  produced in the charged Higgs boson decay. We expect, then, that using only single prong, hadronic  $\tau$  decay modes,  $\tau$ -leptons will be reconstructed with approximately 30% efficiency. However, to be conservative, we assume similar reconstruction efficiencies for the  $t$  and  $\tau$ , and give sensitivity curves for a common set of assumed reconstruction efficiencies. A more complete analysis must include detector efficiency, backgrounds and branching ratios.

How well the signal can be separated from the background depends critically on the  $b$  tagging efficiency which in turn depends on details of the detector. Studies using detector simulations have been performed on related processes. They have found that the efficiency is inversely related to the

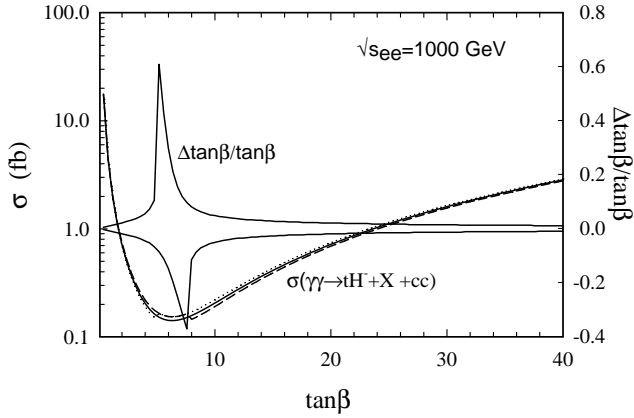


FIG. 4.  $\sigma(\gamma\gamma \rightarrow tH^- + X)$  vs  $\tan\beta$  for the backscattered laser case and the sensitivities to  $\tan\beta$  based only on statistical errors (solid lines) for  $\sqrt{s_{ee}} = 1$  TeV and  $M_H = 200$  GeV. For the cross sections, the solid line represents the expected cross section at the nominal value of  $\tan\beta$ , while the dashed (dotted) line represents the expected cross section at  $\tan\beta - \Delta\tan\beta$  ( $\tan\beta + \Delta\tan\beta$ ).

purity of the  $t$ -quark sample, i.e., the higher the purity the smaller the efficiency. In practice one wants to find the point on this efficiency-purity curve that maximizes the signal to background ratio. Detailed studies on processes similar to the one we are studying use  $b$ -tagging efficiency  $\epsilon \approx 10\%$  for a high purity ( $\geq 90\%$  purity), yet statistically significant sample. Given that it is impossible to know the exact value to use for this important parameter without a real detector with measured properties we give results for different values of the event reconstruction efficiency. With this approach, experimentalists can decide which value most closely corresponds to their detector.

Another consideration is the variation of  $BR(H^\pm \rightarrow tb)$  with  $\tan\beta$  and  $M_{H^\pm}$ , especially for small valued  $\tan\beta$  where the  $tb$  mode competes with the  $\tau\nu$  mode. As noted above, we assume similar reconstruction efficiencies for these two modes and assume that experiments can measure this process through both charged Higgs boson decay modes.

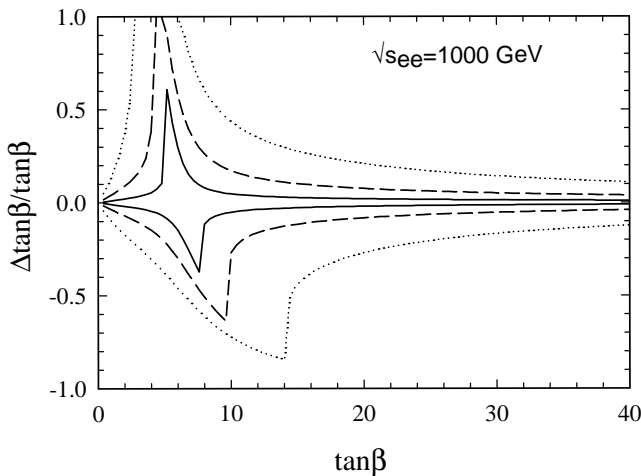


FIG. 5.  $\Delta\tan\beta/\tan\beta$  vs  $\tan\beta$  for the  $\gamma\gamma$  (solid lines),  $e\gamma$  (dashed lines) and  $e^+e^-$  (dotted lines) collider modes for  $\sqrt{s_{ee}} = 1$  TeV and  $M_H = 200$  GeV.

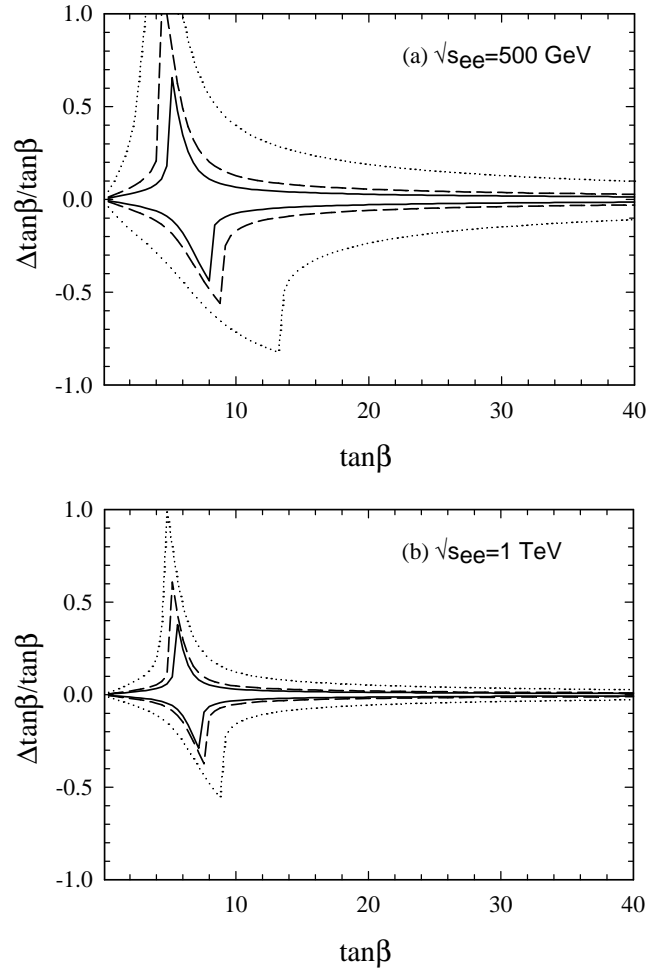


FIG. 6. Sensitivity to  $\tan\beta$  for (a) a  $\sqrt{s_{ee}} = 500$  GeV  $\gamma\gamma$  collider with  $M_H = 100$  GeV (solid line), 150 GeV (dashed line) and 200 GeV (dotted line). (b) A  $\sqrt{s_{ee}} = 1$  TeV  $\gamma\gamma$  collider with  $M_H = 100$  GeV (solid line), 200 GeV (dashed line) and 400 GeV (dotted line).

To obtain our results we assume  $1 \text{ ab}^{-1}$  for the integrated luminosities, the standard used in many LC studies, to estimate event rates and hence statistical errors. We consider 4 center of mass energies appropriate to the various linear collider energies proposed:  $\sqrt{s} = 500, 800, 1000,$  and  $1500$  GeV.

The upper and lower limits on  $\tan\beta$  are obtained as the values of  $\tan\beta \pm \Delta\tan\beta$  for which the cross sections are statistically consistent with the cross sections obtained using the central value of  $\tan\beta$  given on the x-axis. In Fig. 4 we show the cross section versus  $\tan\beta$  along with the  $1\text{-}\sigma$  errors on  $\tan\beta$  presented as the ratio  $\Delta\tan\beta/\tan\beta$ . Over most of the  $\tan\beta$  range there is a strong dependence of the cross section on  $\tan\beta$  so that a precise cross section measurement will result in a good determination of  $\tan\beta$ . However, at  $\tan\beta \approx 6-7$  the cross section is at a minimum so that  $\Delta\sigma/\Delta\tan\beta \sim 0$  resulting in very little sensitivity to  $\tan\beta$  in this region. The minimum of cross section can be seen both numerically and analytically. The matrix element squared, given in Eq. (2), is proportional to  $m_b^2 \tan^2\beta + m_t^2/\tan^2\beta$ ; minimizing this with respect to  $\tan\beta$ , we find  $\tan\beta_{min}$

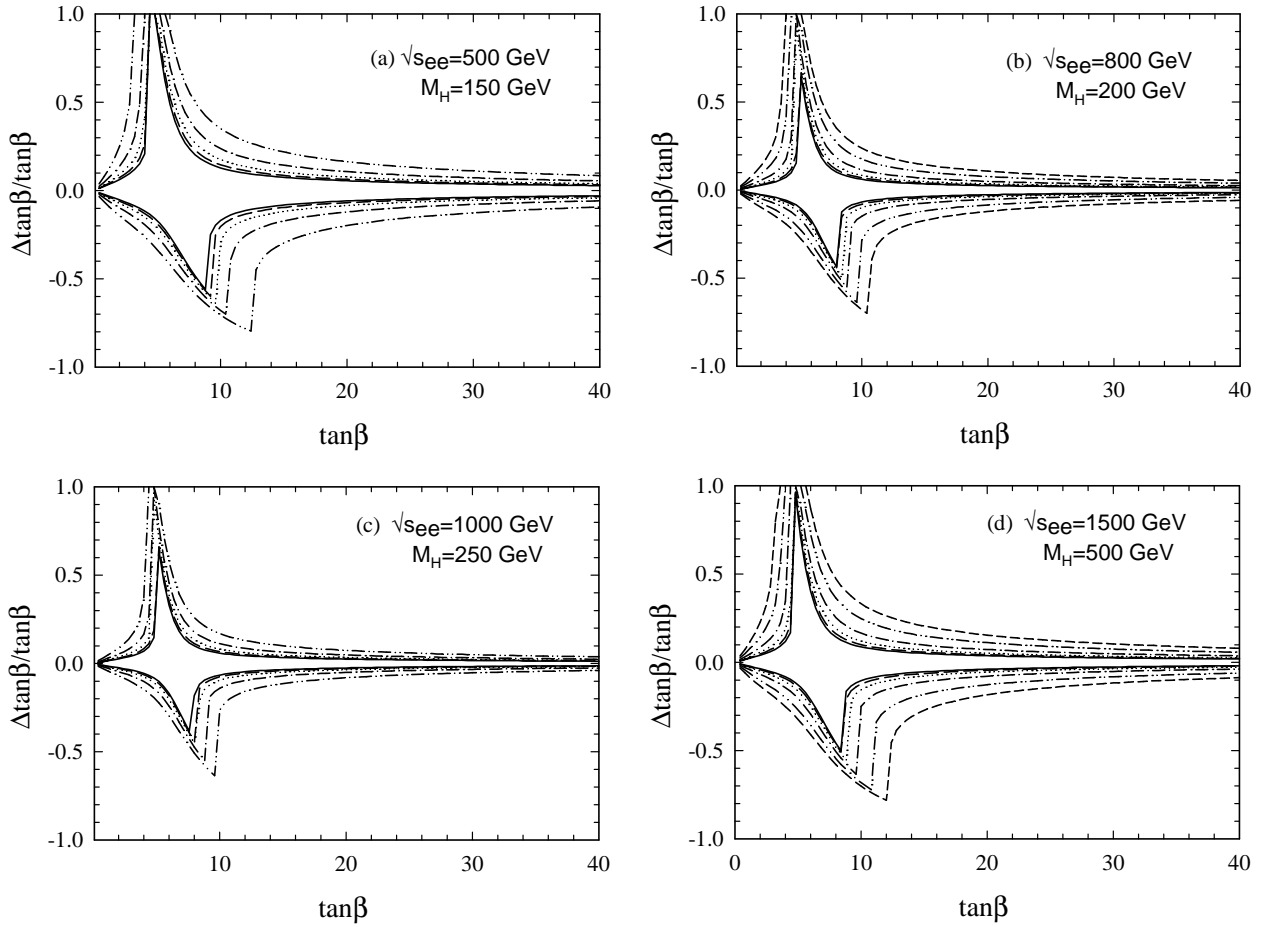


FIG. 7. Sensitivity to  $\tan\beta$  assuming different reconstruction efficiencies for the  $t-H^\pm$  final state.  $\epsilon=100\%$  (solid line),  $75\%$  (dashed line),  $50\%$  (dotted line),  $25\%$  (dot-dashed line),  $10\%$  (dot-dot-dashed line),  $5\%$  (short-dashed line). (a) is for  $\sqrt{s_{ee}}=500$  GeV,  $M_H=150$  GeV; (b) is for  $\sqrt{s_{ee}}=800$  GeV,  $M_H=200$  GeV; (c) is for  $\sqrt{s_{ee}}=1000$  GeV,  $M_H=250$  GeV; and (d) is for  $\sqrt{s_{ee}}=1500$  GeV,  $M_H=500$  GeV.

$=\sqrt{m_t/m_b}\sim 6.3$  for the values of the top and bottom masses used. The actual minimum of sensitivity to  $\tan\beta$  will depend on the detailed behavior of the cross section, but it is no surprise that this process is insensitive to the value of  $\tan\beta\sim 6-7$ . The asymmetry in the sensitivity curves, which is more apparent in subsequent figures, is the simple consequence that when  $\tan\beta\leq 6$ , as  $\tan\beta$  is increased the cross section enters the region least sensitive to  $\tan\beta$  while for  $\tan\beta\geq 6$ , when  $\tan\beta$  is decreased the cross section enters this region.

We have previously pointed out that the measurement of  $\tan\beta$  is much weaker in the  $e\gamma$  and  $e^+e^-$  modes of a future linear collider. In Fig. 5 we show  $\Delta\tan\beta/\tan\beta$  for the  $\gamma\gamma$ ,  $e\gamma$  and  $e^+e^-$  modes for  $\sqrt{s_{ee}}=1$  TeV and  $M_H=200$  GeV. We will henceforth only show results for the  $\gamma\gamma$  case.

As the charged Higgs boson has not yet been observed, its mass is not determined. We expect that the charged Higgs boson will have been discovered and its mass determined by the time this analysis is performed by experimentalists, but for now we allow  $M_H$  to vary. In Fig. 6, we present results on the variation of  $\Delta\tan\beta/\tan\beta$  with  $M_H$  for  $\sqrt{s_{ee}}=500$  GeV and 1 TeV linear colliders operating in  $\gamma\gamma$  mode. The cross section decreases as we near the kinematic limit

$[(M_H+m_t)\sim 0.8\times\sqrt{s_{ee}}]$  as does the sensitivity to the value of  $\tan\beta$ .

The central issue in making a precision measurement of  $\tan\beta$  is the reconstruction efficiency of the signal. Given that this depends on the details of the detector and can only be accurately estimated by performing a detailed detector Monte Carlo simulation in Fig. 7 we show a series of results for reconstruction efficiencies of  $100\%$ ,  $75\%$ ,  $50\%$ ,  $25\%$ ,  $10\%$ , and  $5\%$  for  $\sqrt{s_{ee}}=500$  GeV [Fig. 7(a)],  $800$  GeV [Fig. 7(b)],  $1000$  GeV [Fig. 7(c)] and  $1500$  GeV [Fig. 7(d)]. In this way, when the details of the detector are better known along with a good estimate of the reconstruction efficiency, one can use these figures to estimate the expected measurement error of  $\tan\beta$  and compare the estimate from associated  $t-H^\pm$  production to other processes considered in the literature.

### III. CONCLUSIONS

In this paper we studied the potential for measuring the parameter  $\tan\beta$  arising in type II Higgs doublet models such as MSSM using associated  $t$ -quark charged Higgs boson production in  $\gamma\gamma$  collision;  $\sigma(\gamma\gamma\rightarrow tH^\pm+X)$ . We find that sensitivity to the value of  $\tan\beta$  can be as small as several per-

cent or as large  $\mathcal{O}(100\%)$ , depending on the value of  $\tan\beta$ . For this process, the region of  $\tan\beta\approx 7$  is particularly insensitive to the value of  $\tan\beta$ . Overall, this process is competitive with those considered by Feng and Moroi [21], Barger *et al.* [20], and Gunion *et al.* [18]. Feng and Moroi consider the production of two Higgs bosons,  $HA$  and  $H^+H^-$ , as well as associated  $H^-t\bar{b}$  and find good sensitivity at low  $\tan\beta$ . Barger *et al.* consider associated production of heavy neutral Higgs and heavy quark pairs,  $Hb\bar{b}$ ,  $Ht\bar{t}$ ,  $Ab\bar{b}$  and  $At\bar{t}$ , and also find good sensitivity at low  $\tan\beta$ . Gunion *et al.* also consider Higgs boson associated production with heavy quark pairs, as well as the production of two Higgs bosons,  $HA$  and  $H^+H^-$ , with four heavy quarks in the final state. Their combined analysis indicates that  $\Delta\tan\beta/\tan\beta\sim$  a few to ten percent is possible for  $\tan\beta>30$  and  $\tan\beta<10$ , but there remains a potential hole for intermediate values of

$\tan\beta$ :  $10<\tan\beta<30$ . The analysis considered here provides sensitivity to very low  $\tan\beta\lesssim 3$  and for intermediate to large values of  $\tan\beta\gtrsim 10$ . Thus, it should be considered an additional tool in disentangling the Higgs sector of the electroweak theory and complements other processes previously considered.

#### ACKNOWLEDGMENTS

S.G. thanks Chris Hearty and Peter Zerwas for useful discussions. M.A.D. thanks Zack Sullivan for useful discussions. This research was supported in part by the Natural Sciences and Engineering Research Council of Canada. The work of M.A.D. was supported, in part, by the Commonwealth College of The Pennsylvania State University under a Research Development Grant (RDG).

- 
- [1] For a recent review, see S. Dawson, ICTP Summer School in High-Energy Physics and Cosmology, Miramare, Trieste, Italy, 1998.
- [2] M. Carena and H.E. Haber, *Prog. Part. Nucl. Phys.* **50**, 63 (2003). See also M. Carena *et al.*, "Report of the Higgs Working Group of the Tevatron Run II Supersymmetry/Higgs Workshop," hep-ph/0010338.
- [3] J.F. Gunion, the Proceedings of SUSY02: The 10th International Conference on Supersymmetry and Unification of Fundamental Interactions, 2002 DESY Hamburg, Germany, edited by P. Nath and P.W. Zerwas, Part I, p. 80, hep-ph/0212150.
- [4] For reviews of the MSSM see P. Fayet and S. Ferrara, *Phys. Rep.* **32**, 249 (1977); H.P. Nilles, *ibid.* **110**, 1 (1984); H.E. Haber and G. Kane, *ibid.* **117**, 75 (1985); M. Drees, hep-ph/9611409; X. Tata, in *Boston 1998, Particles, Strings and Cosmology*, edited by P. Nath (World Scientific, Singapore, 1999).
- [5] J.F. Gunion and H. Haber, *Nucl. Phys.* **B272**, 1 (1986); **B402**, 567(E) (1993); **B278**, 449 (1986).
- [6] TESLA Technical Design Report, Part III: Physics at an  $e^+e^-$  Linear Collider, TESLA Report 2001-23, edited by R. D. Heuer, D. Miller, F. Richard, and P. M. Zerwas, 2001.
- [7] A recent review of Higgs boson studies is given by M. Battaglia and K. Desch, in *Batavia 2000, Physics and Experiments with Future Linear  $e^+e^-$  Colliders*, edited by A. Para and H.E. Fisk (AIP, Melville, 2001).
- [8] J.F. Gunion *et al.*, *Phys. Rev. D* **38**, 3444 (1988); A. Djouadi, J. Kalinowski, and P.M. Zerwas, *Z. Phys. C* **57**, 569 (1993); A. Djouadi, J. Kalinowski, P. Ohmann, and P.M. Zerwas, *ibid.* **74**, 93 (1997).
- [9] S. Komamiya, *Phys. Rev. D* **38**, 2158 (1988).
- [10] D. Bowser-Chao, K. Cheung, and S. Thomas, *Phys. Lett. B* **315**, 399 (1993).
- [11] S. Kanemura, S. Moretti, and K. Odagiri, *Eur. Phys. J. C* **22**, 401 (2001); *J. High Energy Phys.* **02**, 011 (2001).
- [12] S. Moretti and S. Kanemura, *Eur. Phys. J. C* **29**, 19 (2003).
- [13] J. Gunion and J. Kelly, *Phys. Rev. D* **56**, 1730 (1997).
- [14] H. Baer, C.-H. Chen, M. Drees, F. Paige, and X. Tata, *Phys. Rev. D* **58**, 075008 (1998); M. Guchait and D.P. Roy, *Phys. Lett. B* **535**, 243 (2002); J.L. Feng, M.E. Peskin, H. Murayama, and X. Tata, *Phys. Rev. D* **52**, 1418 (1995).
- [15] CMS Collaboration, CMS technical proposal, CERN-LHCC-94-38; K.A. Assamagan, Y. Coadou, and A. Deandrea, *Eur. Phys. J. C* **4**, 9 (2002); ATLAS Collaboration, ATLAS Detector and Physics Performance: Technical Design Report, CERN-LHCC-99-14 and CERN-LHCC-99-15; P. Salmi, R. Kinnunen, and N. Stepanov, hep-ph/0301166; S. Moretti and D.P. Roy, *Phys. Lett. B* **470**, 209 (1999); R. Kinnunen, CMS-NOTE-2000-45; S. Slabospitsky, CMS-NOTE-2002-010; S. Banerjee and M. Mainty, *J. Phys. G* **28**, 2443 (2002); K.A. Assamagan, *Acta Phys. Pol. B* **31**, 863 (2000).
- [16] H.-J. He, S. Kanemura, and C.-P. Yuan, *Phys. Rev. Lett.* **89**, 101803 (2002).
- [17] A. Djouadi, J. Kalinowski, and P.M. Zerwas, *Z. Phys. C* **54**, 255 (1992).
- [18] J. Gunion, T. Han, J. Jiang, and A. Sopczak, *Phys. Lett. B* **565**, 42 (2003).
- [19] E. Boos, H.U. Martyn, G. Moortgat-Pick, M. Sachwitz, A. Sherstnev, and P.M. Zerwas, hep-ph/0303110.
- [20] V. Barger, T. Han, and J. Jiang, *Phys. Rev. D* **63**, 075002 (2001).
- [21] J.L. Feng, and T. Moroi, *Phys. Rev. D* **56**, 5962 (1997).
- [22] V. Telnov, *Int. J. Mod. Phys. A* **13**, 2399 (1998).
- [23] M.A. Doncheski and S. Godfrey, *Phys. Rev. D* **67**, 073021 (2003).
- [24] M.A. Doncheski, S. Godfrey, and K.A. Peterson, *Phys. Rev. D* **55**, 183 (1997).
- [25] J.F. Gunion, H.E. Haber, G.L. Kane, and S. Dawson, *The Higgs Hunter's Guide* (Addison-Wesley, Redwood City, CA, 1990).
- [26] V. Barger and R.J. Phillips, *Collider Physics* (Addison-Wesley, Redwood City, CA, 1987).
- [27] I.F. Ginzburg *et al.*, *Nucl. Instrum. Methods Phys. Res.* **205**, 47 (1983); *Nucl. Instrum. Methods Phys. Res. A* **219**, 5 (1984); V.I. Telnov, *ibid.* **294**, 72 (1990); C. Akerlof, Report No. UM-HE-81-59 (unpublished).
- [28] C. Weizsäcker, *Z. Phys.* **88**, 612 (1934); E.J. Williams, *Phys. Rev.* **45**, 729 (1934).

- [29] Particle Data Group, K. Hagiwara *et al.*, Phys. Rev. D **66**, 010001 (2002).
- [30] M. Glück, E. Reya, and A. Vogt, Phys. Lett. B **222**, 149 (1989); Phys. Rev. D **45**, 3986 (1992).
- [31] Two recent reviews are R. Nisius, Phys. Rep. **332**, 165 (2000); M. Krawczyk, A. Zembrzuski, and M. Staszel, *ibid.* **345**, 265 (2001).
- [32] D.W. Duke and J.F. Owens, Phys. Rev. D **26**, 1600 (1982); M. Drees and K. Grassie, Z. Phys. C **28**, 451 (1985); H. Abramowicz, K. Charchula, and A. Levy, Phys. Lett. B **269**, 458 (1991); M. Drees and R. Godbole, Nucl. Phys. **B339**, 355 (1990); M. Glück, E. Reya, and A. Vogt, Phys. Rev. D **46**, 1973 (1992); G.A. Schuler and T. Sjöstrand, Z. Phys. C **68**, 607 (1995); Phys. Lett. B **376**, 193 (1996).
- [33] F. Cornet, P. Jankowski, M. Krawczyk, and A. Lorca, Phys. Rev. D **68**, 014010 (2003).
- [34] A. Djouadi, M. Spira, and P.M. Zerwas, Z. Phys. C **70**, 427 (1996); Phys. Lett. B **311**, 255 (1993); M. Battaglia, hep-ph/9910271.
- [35] A. Djouadi, J. Kalinowski, and P.M. Zerwas, Z. Phys. C **70**, 435 (1996).
- [36] ALEPH Collaboration, R. Barate *et al.*, Phys. Lett. B **414**, 362 (1997); DELPHI Collaboration, P. Abreu *et al.*, *ibid.* **365**, 448 (1996); L3 Collaboration, M. Acciarri *et al.*, *ibid.* **479**, 67 (2000); OPAL Collaboration, G. Alexander *et al.*, *ibid.* **374**, 341 (1996).
- [37] ALEPH Collaboration, A. Heister *et al.*, Eur. Phys. J. C **20**, 401 (2001).
- [38] DELPHI Collaboration, P. Abreu *et al.*, Eur. Phys. J. C **14**, 585 (2000).
- [39] L3 Collaboration, M. Acciarri *et al.*, Phys. Lett. B **429**, 387 (1998).
- [40] OPAL Collaboration, G. Abbiendi *et al.*, Eur. Phys. J. C **21**, 1 (2001).